Tiled QR factorization algorithms

Henricus Bouwmeester, Mathias Jacquelin, Julien Langou, Yves Robert

INSTITUT NATIONAL DE RECHERCHE EN INFORMATIQUE ET EN AUTOMATIQUE

Algorithmes de factorisation QR par blocs

Henricus Bouwmeester — Mathias Jacquelin — Julien Langou — Yves Robert

N° 7601

Avril 2011

Distributed and High Performance Computing

ISSN 0249-6399 ISRN INRIA/RR--7601--FR+ENG

INSTITUT NATIONAL
DE RECHERCHE
EN INFORMATIQUE
ET EN AUTOMATIQUE

INRIA

centre de recherche
GRENOBLE - RHÔNE-ALPES

Algorithmes de factorisation QR par blocs

Henricus Bouwmeester [*] [†] , Mathias Jacquelin [‡] , Julien Langou [*] [§] , Yves Robert [‡] [¶] [‖]

Theme : Distributed and High Performance Computing
Équipe-Projet GRAAL

Rapport de recherche n° 7601 — Avril 2011 — 26 pages

Résumé : Cette étude revisite les algorithmes éxistant pour la factorisation QR de matrices rectangulaires composées de $p \times q$ blocs, où $p \geq q$. Dans ce contexte, nous étudions les chemins critiques et les performances d'algorithmes tels que Sameh-Kuck, Fibonacci, Greedy, ainsi que ceux disponibles dans PLASMA. Bien que ni Fibonacci ni Greedy ne soient optimaux, nous démontrons qu'ils sont tous deux asymptotiquement optimaux pour toutes matrices de taille $p = q^2 f(q)$, où f est une fonction quelconque telle que $\lim_{+\infty} f = 0$. Ce résultat est valide pour toutes matrices dès lors que p et q sont proportionnels, $p = \lambda q$, avec $\lambda \geq 1$, comprenant par là même de nombreuses importantes situations recontrées en pratique (moindre carrés). Nous présentons un grand nombre d'expériences démontrant la supériorité des nouveaux algorithmes pour les matrices ayant significativement plus de lignes que de colonnes.

Mots-clés : Factorisation QR, chemin critique, algorithmes gloutons, matrice ayant significativement plus de lignes que de colonnes

[*] University of Colorado Denver
[†] Research of the first author was fully supported by the National Science Foundation grant # NSF CCF 811520.
[‡] École Normale Supérieure de Lyon
[§] Research of the third author was fully supported by the National Science Foundation grant # NSF CCF 1054864.
[¶] Institut Universitaire de France
[‖] Research of the fourth author was supported in part by the ANR StochaGrid and RESCUE projects.

Centre de recherche INRIA Grenoble – Rhône-Alpes
655, avenue de l'Europe, 38334 Montbonnot Saint Ismier
Téléphone : +33 4 76 61 52 00 — Télécopie +33 4 76 61 52 52

Tiled QR factorization algorithms

Abstract: This work revisits existing algorithms for the QR factorization of rectangular matrices composed of $p \times q$ tiles, where $p \geq q$. Within this framework, we study the critical paths and performance of algorithms such as SAMEH-KUCK, FIBONACCI, GREEDY, and those found within PLASMA. Although neither FIBONACCI nor GREEDY is optimal, both are shown to be asymptotically optimal for all matrices of size $p = q^2 f(q)$, where f is any function such that $\lim_{+\infty} f = 0$. This result applies to all matrices where p and q are proportional, $p = \lambda q$, with $\lambda \geq 1$, thereby encompassing many important situations in practice (least squares). We provide an extensive set of experiments that show the superiority of the new algorithms for tall and skinny matrices.

Key-words: QR factorization, critical path, greedy algorithms, tall and skinny

1 Introduction

Given an m-by-n matrix A with $n \leq m$, we consider the computation of its QR factorization, which is the factorization $A = QR$, where Q is an m-by-n unitary matrix ($Q^H Q = I_n$), and R is upper triangular.

The QR factorization is the time consuming stage of some important numerical computations. The QR factorization of an m-by-n matrix with $n \leq m$ is needed for solving a linear least squares with m equations (observations) and n unknowns. The QR factorization of an m-by-n matrix with $n \leq m$ is used to compute an orthogonal basis (the Q-factor) of the column span of the initial matrix A. For example, all block iterative methods (used to solve large sparse linear systems of equations or computing some relevant eigenvalues of such systems) require orthogonalizing a set of vectors at each step of the process. For these two usage examples, while $n \leq m$, n can range from $n \ll m$ to $n \lessapprox m$. We note that the extreme case $n = m$ is also relevant : the QR factorization of a matrix can be used to solve (square) linear systems of equations (in that case $n = m$). While this requires twice as many flops as an LU factorization, using a QR factorization (a) is unconditionally stable (Gaussian elimination with partial pivoting or pairwise pivoting is not) and (b) avoids pivoting so it may well be faster in some cases (despite requiring twice as many flops).

To obtain a QR factorization, we will consider algorithms which apply a sequence of m-by-m unitary transformations, U_i, ($U_i^H U_i = I$,), $i = 1, \ldots, \ell$, on the left of the matrix A, such that after ℓ transformations the resulting matrix $R = U_\ell \ldots U_1 A$ is upper triangular, in which case, R is indeed the R-factor of the QR factorization. The Q-factor (if needed) can then be obtained by computing $Q = U_1^H \ldots U_\ell^H$. These types of algorithms are in regular use, see for example the LAPACK and ScaLAPACK libraries, and are favored over others algorithms (Cholesky QR or Gram-Schmidt) for their stability.

The unitary transformation U_i is chosen so as to introduce some zeros in the current update matrix $U_{i-1} \ldots U_1 A$. The two basic transformations are Givens rotations and Householder reflections. One Givens rotation introduces one additional zero ; the whole triangularization requires $mn - n(n+1)/2$ Givens rotations for $n < m$. One elementary Householder reflection simultaneously introduces $m - i$ zeros in position $i + 1$ to m in column i ; the whole triangularization requires n Householder reflections for $n < m$. (See LAPACK subroutine *GEQR2*.) The LAPACK *GEQRT* subroutine constructs a compact WY representation to apply a sequence of ib Householder reflections, this enables one to introduce the appropriate zeros in ib consecutive columns and thus leverage optimized Level 3 BLAS subroutines during the update. The blocking of Givens rotations is also possible but is more costly in terms of flops.

The main interest of Givens rotations over Householder transformations is that one can concurrently introduce zeros using disjoint pairs of rows, in other words, two transformations U_i and U_{i+1} may be applicable concurrently. This is not possible using the original Householder reflection algorithm since the transformations work on whole columns and thus does not exhibit this type of intrinsic parallelism forcing this kind of Householder reflections to be applied sequentially. The advantage of Householder reflections over Givens rotations is that, first, Householder reflections perform less flops, and second, the compact WY transformation enables high sequential performance of the algorithm. In a multicore setting, where data locality and parallelism are crucial algorithmic

characteristics for enabling performance, the tiled QR factorization algorithm combines both ideas : use of Householder reflections for high sequential performance and use of a scheme ala Givens rotations to enable parallelism within cores. In essence, either one can think of the tiled QR factorization as a Givens rotation scheme but on tiles (m_b-by-n_b submatrices) instead of on scalars (1-by-1 submatrices) as in the original scheme, or one can think of it as a blocked Householder reflection scheme where each reflection is confined to an extent much less than the full column span, which enables concurrency with other reflections.

Tiled QR factorization in the context of multicore architectures has been introduced in [4, 13, 5]. Initially the focus was on square matrices and the sequence of unitary transformations presented was analogous to Sameh-Kuck [14], which corresponds to reducing the panels with flat trees. The use of binary trees for tall and skinny matrices is explained in [8]. In [10], Hadri et al. propose to combine flat trees and binary trees to handle the intermediate cases. Our theoretical and experimental work explains that we can adapt Greedy [6, 7] to tiles, resulting in better algorithms.

The sequential kernels of the Tiled QR factorization (executed on a core) are made of standard blocked algorithms ala LAPACK encoded in kernels ; the development of these kernels is well understood. The focus of this paper is on improving the overall degree of parallelism of the algorithm. Given a p-by-q tile matrix, we seek to find an appropriate sequence of unitary transformations on the tiled matrix so as to maximize parallelism (minimize critical path length). We will get our inspiration in previous work from the 70s/80s on Givens rotations where the question was somewhat related : given an m-by-n matrix, find an appropriate sequence of Givens rotations as to maximize parallelism. This question is essentially answered in [6, 7, 12, 14] ; we call this class of algorithms "coarse-grain algorithms."

Working with tiles instead of scalars, we introduce four essential differences between the analysis and the reality of the tiled algorithms and the coarse-grain algorithms. First, while there are only two states for a scalar (nonzero or zero), a tile can be in three states (zero, triangle or full). Second, there are more operations available on tiles to introduce zeros ; we have a total of three different tasks which can introduce zeros in a matrix. Third, the factorization and the update are dissociated to enable factorization stages to overlap with update stages. In the coarse-grain algorithm, the factorization and the associated update are considered as a single stage. Fourth and last, while coarse-grain algorithms have only one task, we end up with six different tasks, which have different computational weights ; this dramatically complicates the critical path analysis of the tiled algorithms.

While the Greedy algorithm is optimal for "coarse-grain algorithms", we show that it is not in the case of tiled algorithms. We are unable to devise an optimal algorithm at this point, but we can prove that both Greedy and Fibonacci are asymptotically optimal for all matrices of size $p = q^2 f(q)$, where f is any function such that $\lim_{+\infty} f = 0$. This result applies to all matrices where p and q are proportional, $p = \lambda q$, with $\lambda \geq 1$, thereby encompassing many important situations in practice (least squares).

The paper is organized as follows. Section 2 reviews the numerical kernels needed to perform a tiled QR factorization, and introduces elimination lists, which enable us to formally define tiled algorithms. Section 3 presents the core algorithmic contributions of this paper. One major result is the asymptotic

optimality of two new tiled algorithms, FIBONACCI and GREEDY. Section is devoted to numerical experiments on multicore platforms. For tall and skinny matrices, these experiments confirm the superiority of the new algorithms over state-of-the-art solutions of the PLASMA library [4, 5]. Finally, we provide some concluding remarks in Section 5.

2 The QR factorization algorithm

Tiled algorithms are expressed in terms of tile operations rather than elementary operations. Each tile is of size $n_b \times n_b$, where n_b is a parameter tuned to squeeze the most out of arithmetic units and memory hierarchy. Typically, n_b ranges from 80 to 200 on state-of-the-art machines [2]. Algorithm 1 outlines a naive tiled QR algorithm, where loop indices represent tiles :

Algorithm 1: Naive QR algorithm for a tiled $p \times q$ matrix.

```
for k = 1 to min(p, q) do
    for i = k + 1 to p do
        elim(i, piv(i, k), k)
```

In Algorithm 1, k is the panel index, and $elim(i, piv(i,k), k)$ is an orthogonal transformation that combines rows i and $piv(i,k)$ to zero out the tile in position (i,k). However, this formulation is somewhat misleading, as there is much more freedom for QR factorization algorithms than, say, for Cholesky algorithms (and contrarily to LU elimination algorithms, there are no numerical stability issues). For instance in column 1, the algorithm must eliminate all tiles $(i,1)$ where $i > 1$, but it can do so in several ways. Take $p = 6$. Algorithm 1 uses the transformations

$$elim(2,1,1), elim(3,1,1), elim(4,1,1), elim(5,1,1), elim(6,1,1)$$

But the following scheme is also valid :

$$elim(3,1,1), elim(6,4,1), elim(2,1,1), elim(5,4,1), elim(4,1,1)$$

In this latter scheme, the first two transformations $elim(3,1,1)$ and $elim(6,4,1)$ use distinct pairs of rows, and they can execute in parallel. On the contrary, $elim(3,1,1)$ and $elim(2,1,1)$ use the same pivot row and must be sequentialized. To complicate matters, it is possible to have two orthogonal transformations that execute in parallel but involve zeroing a tile in two different columns. For instance we can add $elim(6,5,2)$ to the previous transformations and run it concurrently with, say, $elim(2,1,1)$. Any tiled QR algorithm will be characterized by an *elimination list*, which provides the ordered list of the transformations used to zero out all the tiles below the diagonal. This elimination list must obey certain conditions so that the factorization is valid. For instance, $elim(6,5,2)$ must follow $elim(6,4,1)$ and $elim(5,4,1)$ in the previous list, because there is a flow dependence between these transformations. Note that, although the elimination list is given as a totally ordered sequence, some transformations can execute in parallel, provided that they are not linked by a dependence : in the

Operation	Panel		Update	
	Name	Cost	Name	Cost
Factor square into triangle	*GEQRT*	4	*UNMQR*	6
Zero square with triangle on top	*TSQRT*	6	*TSMQR*	12
Zero triangle with triangle on top	*TTQRT*	2	*TTMQR*	6

TABLE 1 – Kernels for tiled QR. The unit of time is $\frac{n_b^3}{3}$, where n_b is the blocksize.

example, $elim(6,4,1)$ and $elim(2,1,1)$ could have been swapped, and the elimination list would still be valid.

Before formally stating the conditions that guarantee the validity of (the elimination list of) an algorithm, we explain how orthogonal transformations can be implemented.

2.1 Kernels

To implement a given orthogonal transformation $elim(i, piv(i,k), k)$, one can use six different kernels, whose costs are given in Table 1. In this table, the unit of time is the time to perform $\frac{n_b^3}{3}$ floating-point operations [3].

There are two main possibilities to implement an orthogonal transformation $elim(i, piv(i,k), k)$: The first version eliminates tile (i,k) with the *Triangle on top of square* kernels, as shown in Algorithm 2 :

Algorithm 2: Elimination $elim(i, piv(i,k), k)$ via *Triangle on top of square* kernels.

$GEQRT(piv(i,k), k)$
$TSQRT(i, piv(i,k), k)$
for j $= k+1$ *to* q **do**
  $UNMQR(piv(i,k), k, j)$
  $TSMQR(i, piv(i,k), k, j)$

Here the tile panel $(piv(i,k), k)$ is factored into a triangle (with *GEQRT*). The transformation is applied to subsequent tiles $(piv(i,k), j)$, $j > k$, in row $piv(i,k)$ (with *UNMQR*). Tile (i,k) is zeroed out (with *TSQRT*), and subsequent tiles (i,j), $j > k$, in row i are updated (with *TSMQR*). The flop count is $4 + 6 + (6+12)(q-k) = 10 + 18(q-k)$ (expressed in same time unit as in Table 1). Dependencies are the following :

$$
\begin{array}{ll}
GEQRT(piv(i,k),k) \prec TSQRT(i,piv(i,k),k) & \\
GEQRT(piv(i,k),k) \prec UNMQR(piv(i,k),k,j) & \text{for } j > k \\
UNMQR(piv(i,k),k,j) \prec TSMQR(i,piv(i,k),k,j) & \text{for } j > k \\
TSQRT(i,piv(i,k),k) \prec TSMQR(i,piv(i,k),k,j) & \text{for } j > k
\end{array}
$$

Note that $TSQRT(i, piv(i,k), k)$ and $UNMQR(piv(i,k), k, j)$ can be executed in parallel, as well as *UNMQR* operations on different columns $j, j' > k$. With an unbounded number of processors, the parallel time is thus $4 + 6 + 12 = 22$ time-units.

The second approach to implement the orthogonal transformation $elim(i, piv(i,k), k)$ is with the *Triangle on top of triangle* kernels, as shown in Algorithm 3 :

Algorithm 3: Elimination $elim(i, piv(i,k), k)$ via *Triangle on top of triangle* kernels.

$GEQRT(piv(i,k), k)$
$GEQRT(i,k)$
for j $= k+1$ *to* q **do**
  $UNMQR(piv(i,k), k, j)$
  $UNMQR(i,k,j)$
$TTQRT(i, piv(i,k), k)$
for j $= k+1$ *to* q **do**
  $TTMQR(i, piv(i,k), k, j)$

Here both tiles $(piv(i,k), k)$ and (i,k) are factored into a triangle (with $GEQRT$). The corresponding transformations are applied to subsequent tiles $(piv(i,k), j)$ and (i,j), $j > k$, in both rows $piv(i,k)$ and i (with $UNMQR$). Tile (i,k) is zeroed out (with $TTQRT$), and subsequent tiles (i,j), $j > k$, in row i are updated (with $TTMQR$). The flop count is $2(4+6(q-k))+2+6(q-k) = 10+18(q-k)$, just as before. Dependencies are the following :

$$
\begin{array}{ll}
GEQRT(piv(i,k),k) \prec UNMQR(piv(i,k),k,j) & \text{for } j > k \\
GEQRT(i,k) \prec UNMQR(i,k,j) & \text{for } j > k \\
GEQRT(piv(i,k),k) \prec TTQRT(i,piv(i,k),k) & \\
GEQRT(i,k) \prec TTQRT(i,piv(i,k),k) & \\
TTQRT(i,piv(i,k),k) \prec TTMQR(i,piv(i,k),k,j) & \text{for } j > k \\
UNMQR(piv(i,k),k,j) \prec TTMQR(i,piv(i,k),k,j) & \text{for } j > k \\
UNMQR(i,k,j) \prec TTMQR(i,piv(i,k),k,j) & \text{for } j > k
\end{array}
$$

Now the factor operations in row $piv(i,k)$ and i can be executed in parallel. Moreover, the $UNMQR$ updates can be run in parallel with the $TTQRT$ factorization. Thus, with an unbounded number of processors, the parallel time is $4+6+6 = 16$ time-units.

All the new algorithms introduced in this paper are based on TT (Triangle on top of triangle) kernels. From an algorithmic perspective, TT kernels are more appealing than TS (Triangle on top of square) kernels, as they offer more parallelism. More precisely, we can always break a TS kernel into two TT kernels, replacing a $TSQRT(i, piv(i,k), k)$ (following a $GEQRT(piv(i,k),k)$) by a sequence $GEQRT(i,k)$, $TTQRT(i, piv(i,k), k)$. A similar transformation can be made for the updates. Hence a TS-based tiled algorithm can always be executed with TT-kernels, while the converse is not true. However, the TS kernels provide more data locality, they benefit form a very efficient implementation (see Section 4), and several existing algorithms use these kernels. For all these reasons, and for comprehensiveness, our experiments will compare approaches based on both kernel types.

2.2 Elimination lists

As stated above, any algorithm factorizing a tiled matrix of size $p \times q$ is characterized by its elimination list. Obviously, the algorithm must zero out all tiles below the diagonal : for each tile (i,k), $i > k$, $1 \leq k \leq \min(p,q)$, the list must contain exactly one entry $elim(i, \star, k)$, where $\star$ denotes some row index $piv(i,k)$. There are two conditions for a transformation $elim(i, piv(i,k), k)$ to be valid :

- both rows i and $piv(i,k)$ must be ready, meaning that all their tiles left of the panel (of indices (i,k') and $(piv(i,k),k')$ for $1 \leq k' < k$) must have already been zeroed out : all transformations $elim(i, piv(i,k'), k')$ and $elim(piv(i,k), piv(piv(i,k),k'), k')$ must precede $elim(i, piv(i,k), k)$ in the elimination list
- row $piv(i,k)$ must be a potential annihilator, meaning that tile $(piv(i,k),k)$ has not been zeroed out yet :
  the transformation $elim(piv(i,k), piv(piv(i,k),k), k)$ must follow $elim(i, piv(i,k), k)$ in the elimination list

Any algorithm that factorizes the tiled matrix obeying these conditions is called a *generic tiled algorithm* in the following.

2.3 Execution schemes

In essence, the execution of a generic tiled algorithm is fully determined by its elimination list. This list is statically given as input to the scheduler, and the execution progresses dynamically, with the scheduler executing all required transformations as soon as possible. More precisely, each transformation involves several kernels, whose execution starts as soon as they are ready, i.e., as soon as all dependencies have been enforced.

Recall that a tile (i,k) can be zeroed out only after all tiles (i,k'), with $k' < k$, have been zeroed out. Execution progresses as follows :

- Before being ready for elimination, tile (i,k), $i > k$, must be updated $k-1$ times, in order to zero out the $k-1$ tiles to its left (of index (i,k'), $k' < k$). The last update is a transformation $TTMQR(i, piv(i,k), k-1, k)$ for some row index $piv(i,k)$ such that $elim(i, piv(i,k), k-1)$ belongs to the elimination list. When completed, this transformation triggers the transformation $GEQRT(i,k)$, which can be executed immediately after the completion of the $TTMQR$. In turn, $GEQRT(i,k)$ triggers all the updates $UNMQR(i,k,j)$ for all $j > k$. These updates are executed as soon as they are ready for execution.
- The elimination $elim(i, piv(i,k), k)$ is performed as soon as possible when both rows i and $piv(i,k)$ are ready. Just after the completion of $GEQRT(i,k)$ and $GEQRT(piv(i,k),k)$, the transformation $TTQRT(i, piv(i,k), k)$ is launched. When finished, it triggers the updates $TTMQR(i, piv(i,k), k, j)$ for all $j > k$.

Obviously, the degree of parallelism that can be achieved depends upon the eliminations that are chosen. For instance, if all eliminations in a given column use the same factor tile, they will be sequentialized. This corresponds to the flat tree elimination scheme described below : in each column k, it uses $elim(i,k,k)$ for all $i > k$. On the contrary, two eliminations $elim(i, piv(i,k), k)$ and $elim(i', piv(i',k), k)$ in the same column can be fully parallelized provided

that they involve four different rows. Finally, note that several eliminations can be initiated in different columns simultaneously, provided that they involve different pairs of rows, and that all these rows are ready (i.e., they have the desired number of leftmost zeroes).

The following lemma will prove very useful; it states that we can assume w.l.o.g. that each tile is zeroed out by a tile above it, closer to the diagonal.

Lemma 1. *Any generic tiled algorithm can be modified, without changing its execution time, so that all eliminations* $elim(i, piv(i,k), k)$ *satisfy to* $i > piv(i,k)$.

Démonstration. Define a *reverse* elimination as an elimination $elim(i, piv(i,k), k)$ where $i < piv(i,k)$. Consider a generic tiled algorithm whose elimination list contains some reverse eliminations. Let k_0 be the first column to contain one of them. Let i_0 be the largest row index involved in a reverse elimination in column k_0. The elimination list in column k_0 may contain several reverse eliminations $elim(i_1, i_0, k_0)$, $elim(i_2, i_0, k_0)$, ..., $elim(i_r, i_0, k_0)$, in that order, before row i_0 is eventually zeroed out by the transformation $elim(i_0, piv(i_0, k_0), k_0)$. Note that $piv(i_0, k_0) < i_0$ by definition of i_0. We modify the algorithm by exchanging the roles of rows i_0 and i_1 in column k_0 : the elimination list now includes $elim(i_0, i_1, k_0)$, $elim(i_2, i_1, k_0)$, ..., $elim(i_r, i_1, k_0)$, and $elim(i_1, piv(i_0, k_0), k_0)$. All dependencies are preserved, and the execution time is unchanged. Now the largest row index involved in a reverse elimination in column k_0 is strictly smaller than i_0, and we repeat the procedure until there does not remain any reverse elimination in column k_0. We proceed inductively to the following columns, until all reverse eliminations have been suppressed. □

3 Critical paths

In this section we describe several generic tiled algorithms, and we provide their critical paths, as well as optimality results. These algorithms are inspired by algorithms that have been introduced twenty to thirty years ago [14, 12, 7, 6], albeit for a much simpler, *coarse-grain* model. In this "old" model, the time-unit is the time needed to execute an orthogonal transformation across two matrix rows, regardless of the position of the zero to be created, hence regardless of the length of these rows. Although the granularity is much coarser in this model, any existing algorithm for the old model can be transformed into a generic tiled algorithm, just by enforcing the very same elimination list provided by the algorithm.

Critical paths are obtained using a discrete event based simulator specially developed to this end, based on the Simgrid framework [15]. It carefully handles dependencies across tiles and allows both static and dynamic algorithms. [1]

3.1 Coarse-grain algorithms

We start with a short description of three algorithms for the coarse-grain model. These algorithms are illustrated in Table 2 for a 15×6 matrix.

1. The discrete event based simulator, together with the code for all tiled algorithms, is publicly available at http://graal.ens-lyon.fr/~mjacquel/tiledQR.html

Sameh-Kuck algorithm The SAMEH-KUCK algorithm [14] uses the panel row for all eliminations in each column, starting from below the diagonal and proceeding downwards. Time-steps indicate the time-unit at which the elimination can be done, assuming unbounded resources. Formally, the elimination list is

$$\left\{\Big(elim(i,k,k), i = k+1, k+2, \ldots, p\Big), k = 1, 2, \ldots, \min(p,q)\right\}$$

Fibonacci algorithm The FIBONACCI algorithm is the Fibonacci scheme of order 1 in [12]. Let $coarse(i,k)$ be the time-step at which tile (i,k), $i > k$, is zeroed out. These values are computed as follows. In the first column, there are one 5, two 4's, three 3's, four 2's and four 1's (we would have had five 1's with $p = 16$). Given x as the least integer such that $x(x+1)/2 \geq p-1$, we have $coarse(i,1) = x - y + 1$ where y is the least integer such that $i \leq y(y+1)/2 + 1$. Let the row indices of the z tiles that are zeroed out at step s, $1 \leq s \leq x$, range from i to $i+z-1$. The elimination list for these tiles is $elim(i+j, piv(i+j,1), 1)$, with $piv(i+j) = i+j-z$ for $0 \leq j \leq z-1$. In other words, to eliminate a bunch of z consecutive tiles at the same time-step, the algorithm uses the z rows above them, pairing them in the natural order. Now the elimination scheme of the next column is the same as that of the previous column, shifted down by one row, and adding two time-units : $coarse(i,k) = coarse(i-1,k-1)+2$, while the pairing obeys the same rule.

Greedy algorithm At each step, the GREEDY algorithm [7, 6] eliminates as many tiles as possible in each column, starting with bottom rows. The pairing for the eliminations is done exactly as for FIBONACCI. There is no closed-form formula to compute $coarse(i,k)$, the time-step at which tile (i,k) is eliminated, but it is possible to provide recursive expressions (see [7, 6]).

(a) SAMEH-KUCK						(b) FIBONACCI						(c) GREEDY					
⋆						⋆						⋆					
1	⋆					5	⋆					4	⋆				
2	3	⋆				4	7	⋆				3	6	⋆			
3	4	5	⋆			4	6	9	⋆			3	5	8	⋆		
4	5	6	7	⋆		3	6	8	11	⋆		2	5	7	10	⋆	
5	6	7	8	9	⋆	3	5	8	10	13	⋆	2	4	7	9	12	⋆
6	7	8	9	10	11	3	5	7	10	12	15	2	4	6	9	11	14
7	8	9	10	11	12	2	5	7	9	12	14	2	4	6	8	10	13
8	9	10	11	12	13	2	4	7	9	11	14	1	3	5	8	10	12
9	10	11	12	13	14	2	4	6	9	11	13	1	3	5	7	9	11
10	11	12	13	14	15	2	4	6	8	11	13	1	3	5	7	9	11
11	12	13	14	15	16	1	4	6	8	10	13	1	3	4	6	8	10
12	13	14	15	16	17	1	3	6	8	10	12	1	2	4	6	8	10
13	14	15	16	17	18	1	3	5	8	10	12	1	2	4	5	7	9
14	15	16	17	18	19	1	3	5	7	10	12	1	2	3	5	6	8

TABLE 2 – Time-steps for coarse-grain algorithms.

Consider a rectangular $p \times q$ matrix, with $p > q$. With the coarse-grain model, the critical path of SAMEH-KUCK is $p+q-2$, and that of FIBONACCI is $x+2q-2$, where x is the least integer such that $x(x+1)/2 \geq p-1$. The critical path of GREEDY is unknown, but two important results are known : (i) the critical path of GREEDY is optimal; (ii) its value tends to $2q$ if p is negligible in front of q^2, i.e., if we have $p = q^2 f(q)$ where f is any function such that $\lim_{+\infty} f = 0$ (and $f(q) > 1/q$ so that $p > q$). In particular, let p and q be proportional, $p = \lambda q$, with a constant $\lambda > 1$: FIBONACCI is asymptotically optimal, because x is of the order of $\sqrt{q}$, hence its critical path is $2q + o(q)$. On

the contrary, SAMEH-KUCK is not asymptotically optimal since its critical path is $(1+\lambda)q-2$. For square $q \times q$ matrices, critical paths are slightly different ($2q-3$ for SAMEH-KUCK, $x+2q-4$ for FIBONACCI), but the important result is that all three algorithms are asymptotically optimal in that case.

3.2 Tiled algorithms

As stated above, each coarse-grain algorithm can be transformed into a tiled algorithm, simply by keeping the same elimination list, and triggering the execution of each kernel as soon as possible. However, because the weights of the factor and update kernels are not the same, it is much more difficult to compute the critical paths of the transformed (tiled) algorithms. Table 3 is the counterpart of Table 2, and depicts the time-steps at which tiles are actually zeroed out. Note that the tiled version of SAMEH-KUCK is indeed the FLATTREE algorithm in PLASMA [4, 5], and we have renamed it accordingly. As an example, Algorithm 4 shows the GREEDY algorithm for the tiled model.

(a) SAMEH-KUCK

⋆					
6	⋆				
8	28	⋆			
10	34	50	⋆		
12	40	56	72	⋆	
14	46	62	78	94	⋆
16	52	68	84	100	116
18	58	74	90	106	122
20	64	80	96	112	128
22	70	86	102	118	134
24	76	92	108	124	140
26	82	98	114	130	146
28	88	104	120	136	152
30	94	110	126	142	158
32	100	116	132	148	164

(b) FIBONACCI

⋆					
14	⋆				
12	48	⋆			
12	46	70	⋆		
10	42	68	92	⋆	
10	40	64	90	114	⋆
10	40	62	86	112	136
8	36	62	84	108	134
8	34	58	84	106	130
8	34	56	80	106	128
8	34	56	78	102	128
6	28	56	78	100	122
6	28	50	78	100	122
6	28	44	72	100	122
6	22	44	60	94	116

(c) GREEDY

⋆					
12	⋆				
10	42	⋆			
10	40	64	⋆		
8	36	62	86	⋆	
8	34	56	84	106	⋆
8	34	56	78	102	128
8	30	52	78	100	122
6	28	50	72	100	118
6	28	50	72	94	116
6	28	50	68	94	116
6	28	44	66	88	110
6	22	44	66	88	110
6	22	44	60	82	104
6	22	38	60	76	98

(d) BINARYTREE

⋆					
6	⋆				
8	28	⋆			
6	36	56	⋆		
10	34	70	90	⋆	
6	44	68	104	124	⋆
8	28	78	102	138	158
6	42	62	112	136	172
12	40	76	96	146	170
6	46	74	110	130	180
8	28	80	108	144	164
6	36	56	114	142	178
10	34	64	84	148	176
6	38	62	92	112	182
8	28	66	90	114	134

(e) PLASMATREE ($BS = 5$)

⋆					
6	⋆				
8	28	⋆			
10	34	50	⋆		
12	40	56	72	⋆	
14	46	62	78	94	⋆
6	54	74	90	106	122
8	28	82	102	118	134
10	34	50	110	130	146
12	40	56	72	138	158
16	52	68	84	100	166
6	56	80	96	112	128
8	28	84	108	124	140
10	34	50	112	136	152
12	40	56	72	140	164

TABLE 3 – Time-steps for tiled algorithms.

A first (and quite unexpected) result is that GREEDY is no longer optimal, as shown in the first two columns of Table 3(a) for a 15×2 matrix. In each column and at each step, **the ASAP algorithm** starts the elimination of a tile as soon as there are at least two rows ready for the transformation. When $s \geq 2$ eliminations can start simultaneously, ASAP pairs the $2s$ rows just as FIBONACCI and GREEDY, the first row (closest to the diagonal) with row $s+1$, the second row with row $s+2$, and so on. As a matter of a fact, when processing the second column, both ASAP and GREEDY begin with the elimination of lines 10 to 15 (at time step 20). However, once tiles $(13,2)$, $(14,2)$ and $(15,2)$ are zeroed out (i.e. at time step 22), ASAP eliminates 4 zeros, in rows 9 through 12. On the contrary, GREEDY waits until time step 26 to eliminate 6 zeros in rows 6 through 12. In a sense, ASAP is the counterpart of GREEDY at the tile level. However, ASAP is not optimal either, as shown in Table 3(a) for a 15×3 matrix. On larger examples, the critical path of GREEDY is better than that of ASAP, as shown in Table 3(b).

We have a closed-form formula for the critical path of tiled FLATTREE, but not for that of tiled FIBONACCI (contrarily to the coarse-grain case). But we provide an asymptotic expression, both for FIBONACCI and for GREEDY. More importantly, we show that both tiled algorithms remain asymptotically optimal. We state our main result :

Theorem 1. *Consider a tiled matrix of size $p \times q$, where $p \geq q$:*

Algorithm 4: GREEDY algorithm via *Triangle on top of triangle* kernels.

```
for j = 1 to q do
    /* nz(j) is the number of tiles which have been eliminated
       in column j                                              */
    nZ(j) = 0
    /* nT(j) is the number of tiles which have been
       triangularized in column j                               */
    nT(j) = 0
while column q is not finished do
    for j = q down to 1 do
        if j == 1 then
            /* Triangularize the first column if not yet done */
            nT_new = nT(j) + (p − nT(j))
            if p − nT(j) > 0 then
                for k = p down to 1 do
                    GEQRT(k, j)
                    for jj = j + 1 to q do
                        UNMQR(k, j, jj)
        else
            /* Triangularize every tile having a zero in the
               previous column                                  */
            nT_new = nZ(j − 1)
            for k = nT(j) to nT_new − 1 do
                GEQRT(p − k, j)
                for jj = j + 1 to q do
                    UNMQR(p − k, j, jj)
        /* Eliminate every tile triangularized in the previous
           step                                                 */
        nZ_new = nZ(j) + ⌊(nT(j) − nZ(j)) / 2⌋
        for kk = nZ(j) to nZ_new − 1 do
            piv(p − kk) = p − kk − nZ_new + nZ(j)
            TTQRT(p − kk, piv(p − kk), j)
            for jj = j + 1 to q do
                TTMQR(p − kk, piv(p − kk), j, jj)
        /* Update the number of triangularized and eliminated
           tiles at the next step                           */
        nT(j) = nT_new
        nZ(j) = nZ_new
```

(a) GREEDY nor ASAP are optimal.

(a) GREEDY			(b) ASAP		
⋆			⋆		
12	⋆		12	⋆	
10	42	⋆	10	40	⋆
10	40	64	10	36	86
8	36	62	8	34	80
8	34	56	8	32	74
8	34	56	8	30	68
8	30	52	8	28	62
6	28	50	6	28	56
6	28	50	6	26	50
6	28	50	6	24	46
6	28	44	6	24	44
6	22	44	6	22	44
6	22	44	6	22	40
6	22	38	6	22	38

(b) GREEDY generally outperforms ASAP.

		q			
p	Algorithm	16	32	64	128
16	GREEDY	310			
	ASAP	310			
32	GREEDY	360	650		
	ASAP	402	656		
64	GREEDY	374	726	1342	
	ASAP	588	844	1354	
128	GREEDY	396	748	1452	2732
	ASAP	966	1222	1748	2756

TABLE 4 – Neither GREEDY nor ASAP are optimal.

1. *The critical path length for* FLATTREE *is* $2p+2$ *if* $p \geq q = 1$, $6p+16q-22$ *if* $p > q > 1$ *and* $22q - 24$ *if* $p = q > 1$
2. *The critical path length of* FIBONACCI *is at most* $22q + 6\lceil\sqrt{2p}\rceil$, *and that of* GREEDY *is at most* $22q + 6\lceil\log_2 p\rceil$
3. *The optimal critical path length is at least* $22q - 30$
4. FIBONACCI *is asymptotically optimal if* $p = q^2 f(q)$, *where* $\lim_{+\infty} f = 0$
5. GREEDY *is asymptotically optimal if* $\log_2 p = q f(q)$, *where* $\lim_{+\infty} f = 0$

Démonstration. **Proof of (1).** Consider first the case $p \geq q = 1$. We shall proceed by induction on p to show that the critical path of FLATTREE is of length $2p + 2$, If $p = 1$, then from Table 1 the result is obtained since only $GEQRT(1, 1)$ is required. With the base case established, now assume that this holds for all $p - 1 > q = 1$. Thus at time $t = 2(p - 1) + 2 = 2p$, we have that for all $p - 1 \geq i \geq 1$ tile $(i, 1)$ has been factorized into a triangle and for all $p-1 \geq i > 1$, tile $(i, 1)$ has been zeroed out. Therefore, tile $(p, 1)$ will be zeroed out with $TTQRT(p, 1)$ at time $t + 2 = 2(p - 1) + 2 + 2 = 2p + 2$.

Consider now the case $p > q > 1$. We show by induction on k that tile (i, k), for $i > k \geq 2$, is zeroed out in FLATTREE at time unit $6i + 16k - 22$. For $k = 2$, tile $(2, 2)$ is updated from step $k = 1$ at time $4 + 6 + 6 = 16$, and it is factored into a triangle at time 20. Tile $(3, 2)$ is updated from step $k = 1$ at time 22 factored into a triangle at time 26 and then zeroed out at time $26 + 2 = 28 = 6 \times 3 + 16 \times 2 - 22$. A new tile in column 2 is zeroed out every 6 time units, hence the initialization of the induction for $k = 2$. Assume now that the formula holds up to column k, and let $t = 6(k + 1) + 16k - 22$ be the time at which tile $(k + 1, k)$ is zeroed out. Tile $(k + 1, k + 1)$ is updated from step k at time $t - 2 + 6 + 6 = t + 10$ and factored into a triangle at time $t + 14$. By induction, tile $(k+2, k)$ is zeroed out at time $t+6$, hence triangularized at time $t+4$. The corresponding $UNMQR$ update of tile $(k+2, k+1)$ ends at time $t+10$, its $TTMQR$ update ends at time $\max(t + 14, t + 10) + 6 = t + 20$. Hence tile $(k + 2, k + 1)$ can indeed be zeroed out at time $\max(t + 12, t + 20) + 2 = t + 22$.

A new tile in column $k+1$ can be zeroed out every 6 time units, hence the induction formula for $k+1$.

Finally, for a square matrix of size $q \times q$, consider the above formula for a rectangular matrix with $p = q+1$. Instead of zeroing out the last tile $(q+1, q)$ with tile (q, q), simply need to factor tile (q, q) into a triangle with $GEQRT(q, q)$. This costs 4 time units instead of 6 when adding $TTQRT(q+1, q, q)$, and explains the difference of 2 in the formula for square matrices.

Proof of (2). FIBONACCI and GREEDY are more difficult to analyze than FLATTREE, but we provide an upper bound of their critical path. The approach is the same for both algorithms, and hereafter ALG denotes either FIBONACCI or GREEDY. Let $coarse(i, k)$ be the time-step at which tile (i, k) is zeroed out in ALG with the coarse-grain model (see Table 2 for examples). We derive a "slowed down" version of the tiled version of ALG by terminating the zeroing out of tile (i, k) at time-step

$$6\,coarse(2, 1) + 22(k-1) - 6(coarse(k, k) - coarse(i, k)).$$

We say that this version is slowed down because we do not start the zeroing out of the tiles as soon as possible. For instance in the first column, tile $(i, 1)$ is zeroed out at time $6\,coarse(i, k)$, which is larger than the value given in Table 3. However, we keep the same elimination list as in the original version of ALG, and we trigger the update and factor operations as soon as possible when the zeroing out operation is completed. We only delay these latter operations.

The intuitive idea for delaying the eliminations is that the corresponding updates will be fully overlapped, within a given column, or when proceeding from one column to the next : in this case, allowing for a time-shift of 22 smooths the chaining of the updates. The regular and repetitive spacing of the eliminations allows us to check (just as we did to prove (1)) that all dependencies are enforced in the slowed down version of ALG. Because the case-analysis is tedious, we have written a program for a sanity check of the validity of ALG [2].

In the coarse-grain model, ALG terminates the first column in time x, so the critical path of its slowed down version is $6x + 22(q-1)$. For FIBONACCI, x is the least integer such that $x(x+1)/2 \geq p-1$, hence $x \leq \lceil \sqrt{2p} \rceil$. For GREEDY, $x = \lceil \log_2(p-1) \rceil \leq \lceil \log_2 p \rceil$, hence the result.

Proof of (3). Consider a square $q \times q$ matrix B, with $q \geq 2$. Assume that there are only three non-zero sub-diagonals, i.e., that tile (i, k) is initially zero in B for $i > k+3$. Because there are only three non-zero tiles below the diagonal, there is a constant number of possible row pairings in each column. An exhaustive search is to try all possible pairings in the first column, followed by all possible pairings in the second column, and so on. After a few columns, a pattern emerges, and we can identify that any optimal algorithm (there are several of them) needs at least 22 time-steps to proceed from one column to the next. It is possible to save a few steps at the beginning and end of the execution, and the optimal critical path is $22q - 30$. Here also, because the case-analysis is long and tedious, we have written a program for a sanity check of the latter value.

Now we show that the optimal critical path for a general $p \times q$ matrix A, with $p \geq q \geq 2$, is at least equal to the critical path of the previous $q \times q$ matrix

2. All program sources are publicly available at http://graal.ens-lyon.fr/~mjacquel/tiledQR.html

B with three sub-diagonals. Indeed, Lemma 1 shows that there exist optimal algorithms for factoring A without any reverse elimination. Consider such an algorithm, and discard all eliminations that involve zeroing out elements below the third sub-diagonal, or outside the $q \times q$ top square : the critical path cannot increase, and we have an elimination scheme for B, which proves the desired result.

Note that using B instead of A is the key to the proof : in each column of B, there is only a constant number of possible row pairings, which makes it possible to try all combinations for several consecutive columns. Reasoning with A instead would need a completely different proof (yet to be invented).

Proof of (4) and (5). These are a direct consequence of (3) an (4). □

In Table 3 we also report time-steps for the BinaryTree algorithm in PLASMA [8]. As its name indicates, this algorithm performs a binary tree reduction to zero out tiles in each column. Here is an asymptotic expression of its critical path :

Proposition 1. *Consider a tiled matrix of size $p \times q$, where $p \geq q$. The critical path length of* BinaryTree *is $6q \log_2 p + o(q \log_2 p)$.*

Démonstration. It is possible to derive an exact expression for the critical path length of BinaryTree in the special case where p and q are both exact powers of two, with $q < p$. We obtain the value $(10 + 6 \log_2 p)q - 4 \log_2 p - 6$. As before, the proof goes by (tedious) induction. Here also, we have written a program for a sanity check of the latter value. The asymptotic value follows easily for an arbitrary matrix, by enlarging each dimension to the nearest power of two. □

Proposition 1 shows that BinaryTree is not asymptotically optimal, but performs best for tall and skinny matrices. The PLASMA library provides more algorithms, that can be informally described as trade-offs between FlatTree and BinaryTree. These algorithms are referred to as PlasmaTree in all the following, and differ by the value of an input parameter called the *domain size* BS. This domain size can be any value between 1 and q, inclusive. Within a domain, that includes BS consecutive rows, the algorithm works just as FlatTree : the first row of each domain acts as a local panel and is used to zero out the tiles in all the other rows of the domain. Then the domains are merged : the panel rows are zeroed out by a binary tree reduction, just as in BinaryTree. As the algorithm progresses through the columns, the domain on the very bottom is reduced accordingly, until such time that there is one less domain. For the case that $BS = 1$, PlasmaTree follows a binary tree on the entire column, and for $BS = q$, the algorithm executes a flat tree on the entire column. It seems very difficult for a user to select the domain size BS leading to best performance, but it is known that BS should increase as q increases. In Table 3, we depict the time-steps of PlasmaTree with a domain size of $BS = 5$. In the experiments of Section 4, we use all possible values of BS and retain the one leading to the best value.

4 Experimental results

All experiments were performed on a 48-core machine composed of eight hexa-core AMD Opteron 8439 SE (codename Istanbul) processors running at

2.8 GHz. Each core has a theoretical peak of 11.2 Gflop/s with a peak of 537.6 Gflop/s for the whole machine. The Istanbul micro-architecture is a NUMA architecture where each socket has 6 MB of level-3 cache and each processor has a 512 KB level-2 cache and a 128 KB level-1 cache. After having benchmarked the AMD ACML and Intel MKL BLAS libraries, we selected MKL (10.2) since it appeared to be slightly faster in our experimental context. Linux 2.6.32 and Intel Compilers 11.1 were also used in conjunction with PLASMA 2.3.1.

For all results, we show both double and double complex precision, using all 48 cores of the machine. The matrices are of size $m = 8000$ and $200 \leq n \leq 8000$. The size of the tiles is kept constant at $n_b = 200$, so that the matrices can also be viewed as $p \times q$ tiled matrices where $p = 40$ and $1 \leq q \leq 40$. All kernels use an inner blocking parameter of $i_b = 32$.

The PLASMA interface allows one to specify the dependencies between tasks by designating the data as either INPUT, OUTPUT, INOUT, or NODEP. In our experimental context, we found that the update kernels (*UNMQR*, *TTMQR*, and *TSMQR*) introduced false dependencies between the tasks which sequentializes the execution of update with the factorization kernels *TTQRT* or *TSQRT*. In order to alleviate these, we altered the dependency designation within each of the update kernels for the matrix of Householder reflectors, V, from INPUT to NODEP as is further explained in [11]. The dependencies between the tasks are still consistent since the T matrix within each update kernel continues to be designated as INPUT so that any subsequent task which overwrites this T matrix cannot be executed.

For each experiment, we provide a comparison of the theoretical performance to the actual performance. The theoretical performance is obtained by modeling the limiting factor of the execution time as either the critical path, or the sequential time divided by the number of processors. This is similar in approach to the Roofline model [17]. Taking γ_{seq} as the sequential performance, T as the total number of flops, cp as the length of the critical path, and P as the number of processors, the predicted performance, γ_{pred}, is

$$\gamma_{pred} = \frac{\gamma_{seq} \cdot T}{\max\left(\frac{T}{P}, cp\right)}$$

Figures **??** and **??** depict the predicted performance of all algorithms which use the *Triangle on top of triangle* kernels. For double complex precision, sequential kernels reach 3.1860 GFlop/s while in double precision, the peak performance is 3.8440 GFlop/s. Since PlasmaTree provides an additional tuning parameter of the domain size, we show the results for each value of this parameter as well as the composition of the best of these domain sizes. Again, it is not evident what the domain size should be for the best performance, hence our exhaustive search.

Part of our comprehensive study also involved comparisons made to the Semi-Parallel Tile and Fully-Parallel Tile CAQR algorithms found in [9] which are much the same as those found in PLASMA. As with PLASMA, the tuning parameter *BS* controls the domain size upon which a flat tree is used to zero out tiles below the root tile within the domain and a binary tree is used to merge these domains. Unlike PLASMA, it is not the bottom domain whose size decreases as the algorithm progresses through the columns, but instead is the top domain. In this study, we found that the PLASMA algorithms performed

identically or better than these algorithms and therefore have not presented these comparisons.

Figure **??** and **??** illustrate the experimental performance reached by GREEDY, FIBONACCI and PLASMATREE algorithms using the *Triangle on top of triangle* kernels. In both cases, double or double complex precision, the performance of GREEDY is better than PLASMATREE even for the best choice of domain size. Moreover, as expected from the analysis in Section 3.2, GREEDY outperforms FIBONACCI the majority of the time. Furthermore, we see that, for rectangular matrices, the experimental performance in double complex precision matches the prediction. This is not the case for double precision because communications have higher impact on performance.

While it is apparent that GREEDY does achieve higher levels of performance, the percentage may not be as obvious. To that end, taking GREEDY as the baseline, we present in Figure **??** the theoretical, double, and double complex precision overhead for each algorithm that uses the *Triangle on top of triangle* kernel as compared to GREEDY. These overheads are respectively computed in terms of critical path length and time. At a smaller scale (Figure **??**), it can be seen that GREEDY can perform up to 13.6% better than PLASMATREE.

For all matrix sizes considered, $p = 40$ and $1 \leq q \leq 40$, in the theoretical model, the critical path length for GREEDY is either the same as that of PLASMATREE ($q = 1$) or is up to 25% shorter than PLASMATREE ($q = 6$). Analogously, the critical path length for GREEDY is at least 2% to 27% shorter than that of FIBONACCI. In the experiments, the matrix sizes considered were $p = 40$ and $q \in \{1, 2, 4, 5, 10, 20, 40\}$. In double precision, GREEDY has a decrease of at most 1.5% than the best PLASMATREE ($q = 1$) and a gain of at most 12.8% than the best PLASMATREE ($q = 5$). In double complex precision, GREEDY has a decrease of at most 1.5% than the best PLASMATREE ($q = 1$) and a gain of at most 13.6% than the best PLASMATREE ($q = 2$). Similarly, in double precision, GREEDY provides a gain of 2.6% to 28.1% over FIBONACCI and in double complex precision, GREEDY has a decrease of at most 2.1% and a gain of at most 28.2% over FIBONACCI.

Although it is evidenced that PLASMATREE does not vary too far from GREEDY or FIBONACCI, one must keep in mind that there is a tuning parameter involved and we choose the best of these domain sizes for PLASMATREE to create the composite result, whereas with GREEDY, there is no such parameter to consider. Of particular interest is the fact that GREEDY always performs better than any other algorithm [3] for $p \gg q$. In the scope of PLASMATREE, a domain size $BS = 1$ will force the use of a binary tree so that both GREEDY and PLASMATREE behave the same. However, as the matrix tends more to a square, i.e., q tends toward p, we observe that the performance of all of the algorithms, including FLATTREE, are on par with GREEDY. As more columns are added, the parallelism of the algorithm is increased and the critical path becomes less of a limiting factor, so that the performance of the kernels is brought to the forefront. Therefore, all of the algorithms are performing similarly since they all share the same kernels.

In order to correctly assess the impacts of the kernel selection towards the performance of the algorithms, Figures **??** and **??** show both the in cache and

3. When $q = 1$, GREEDY and FLATTREE exhibit close performance. They both perform a binary tree reduction, albeit with different row pairings.

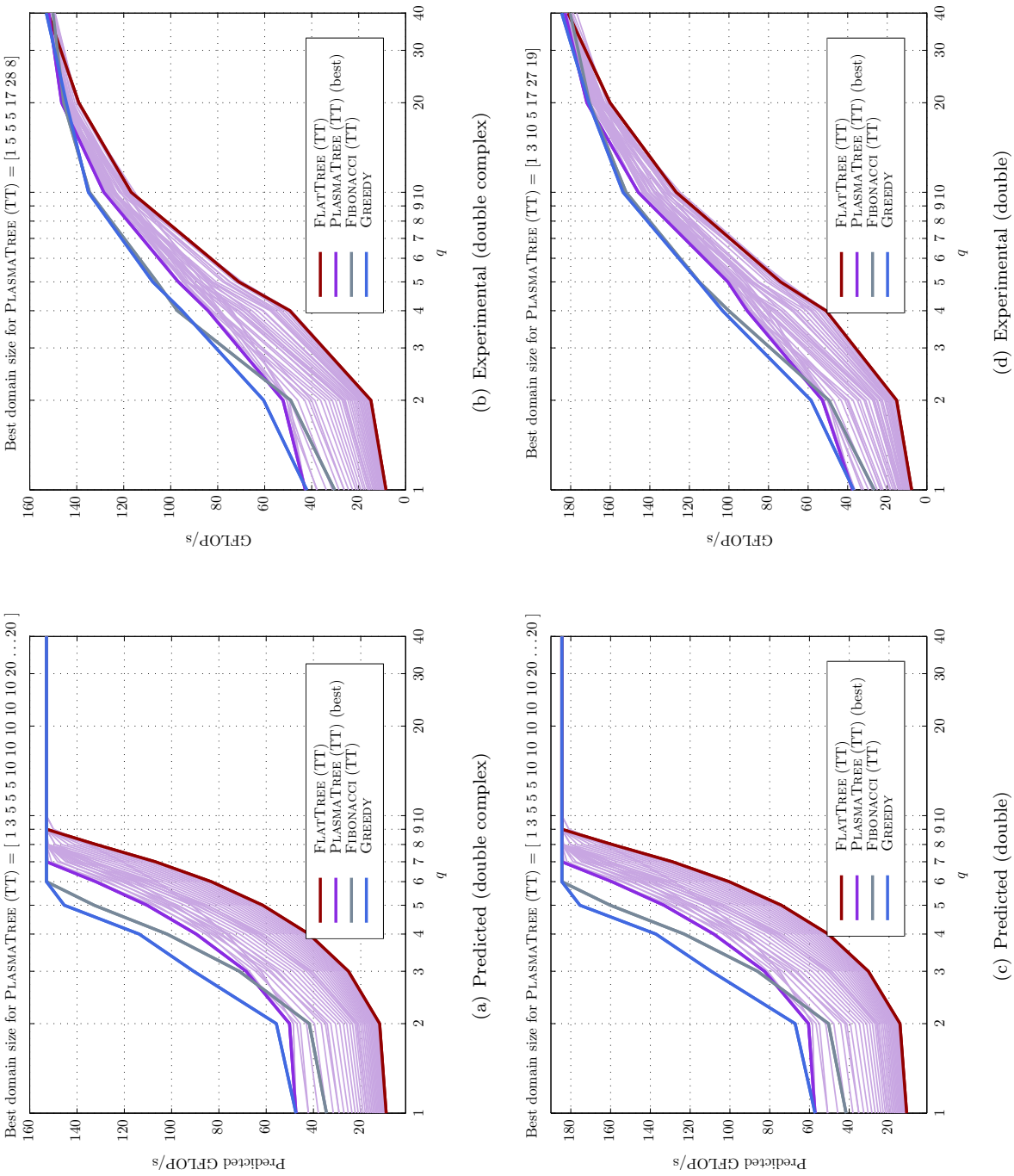

(a) Predicted (double complex)

(b) Experimental (double complex)

(c) Predicted (double)

(d) Experimental (double)

FIGURE 1 – Predicted and experimental performance of QR factorization - *Triangle on top of triangle* kernels

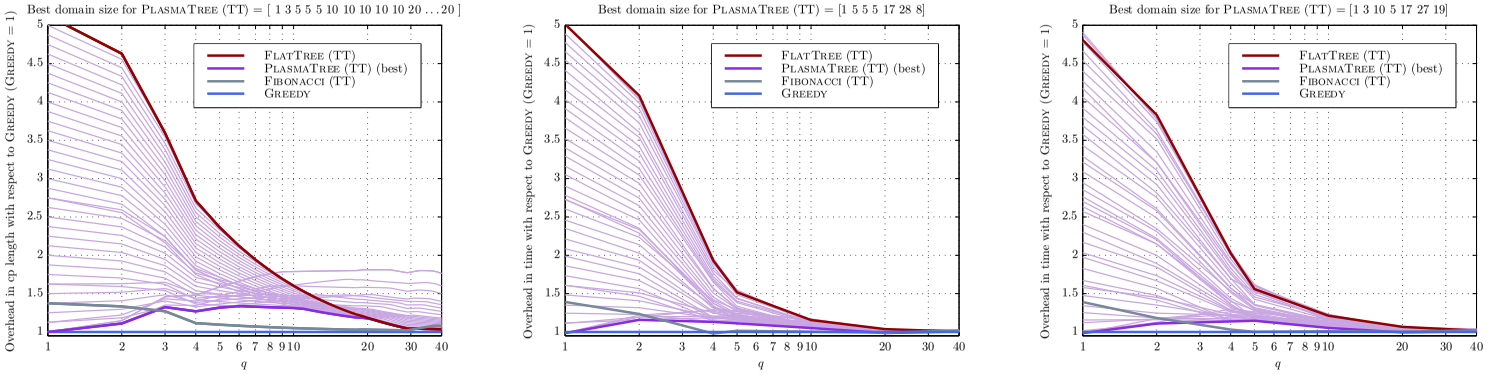

(a) Theoretical CP length (b) Experimental (double complex) (c) Experimental (double)

FIGURE 2 – Overhead in terms of critical path length and time with respect to GREEDY (GREEDY = 1)

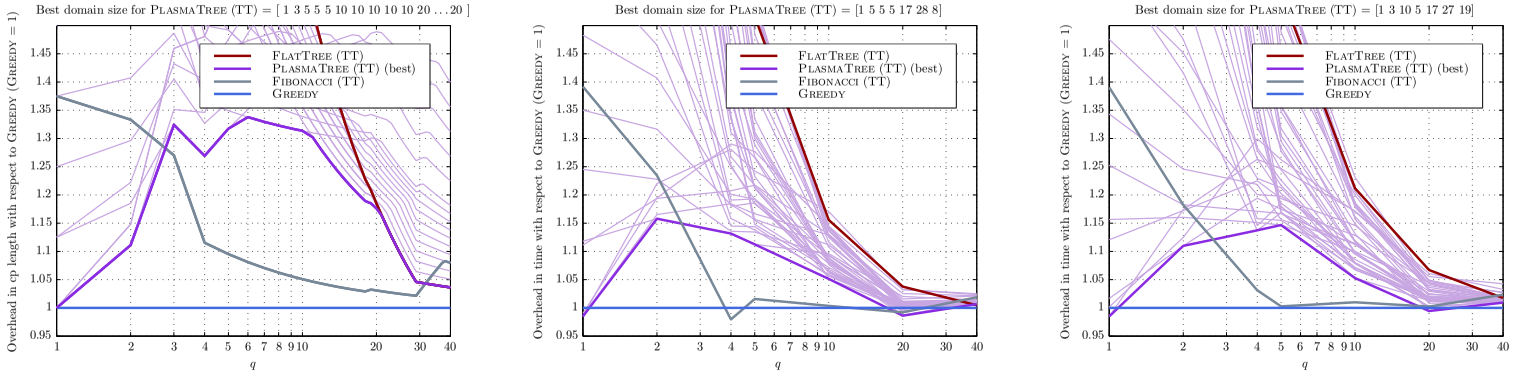

(a) Theoretical CP length (b) Experimental (double complex) (c) Experimental (double)

FIGURE 3 – Detailed view of the overhead in terms of critical path length and time with respect to GREEDY (GREEDY = 1)

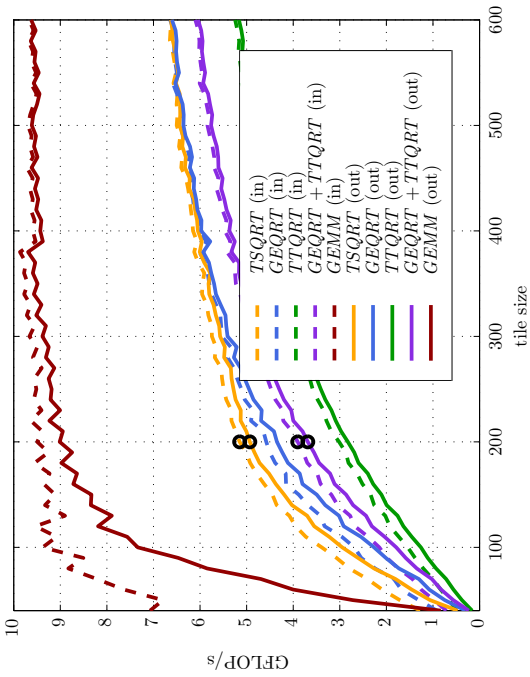

(a) Factorization kernels

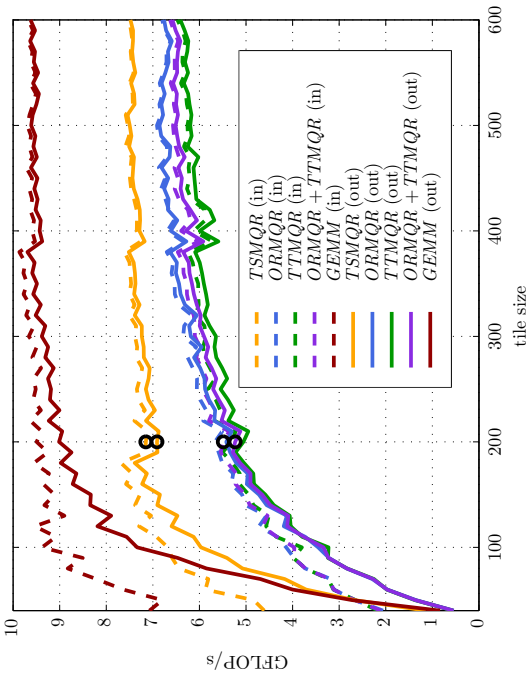

(b) Update kernels

FIGURE 5 – Kernel performance for double precision

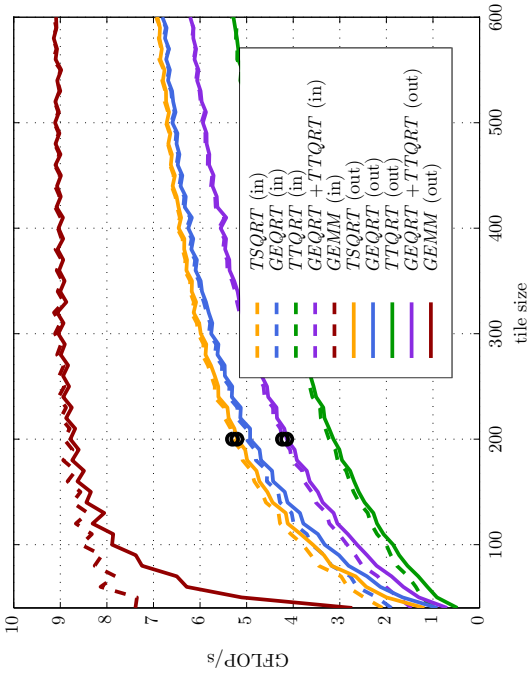

(a) Factorization kernels

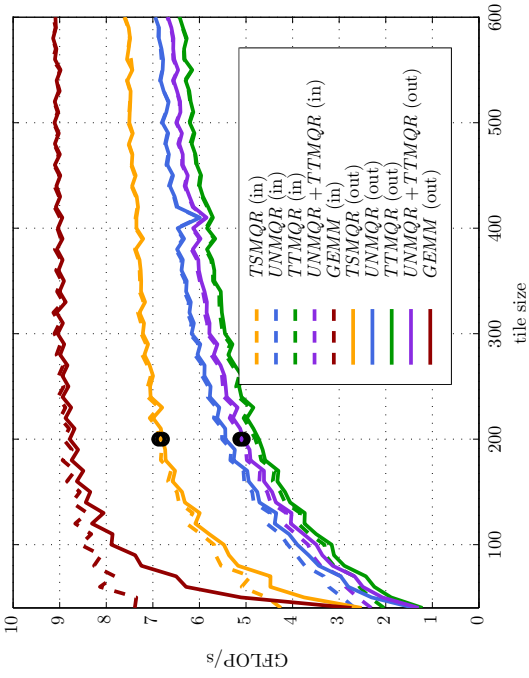

(b) Update kernels

FIGURE 4 – Kernel performance for double complex precision

out of cache performance using the *No Flush* and *MultCallFlushLRU* strategies as presented in [1, 16]. Since an algorithm using the *Triangle on top of triangle* kernel will need to call *GEQRT* as well as *TTQRT* to achieve the same as *TSQRT*, the comparison is made between *GEQRT* + *TTQRT* and *TSQRT*. For $n_b = 200$, the observed ratio for in cache kernel speed for *TSQRT* to *GEQRT* + *TTQRT* is 1.3374 and for *TSMQR* to *UNMQR* + *TTMQR* is 1.3207 while for out of cache the ratio for *TSQRT* to *GEQRT* + *TTQRT* is 1.3193 and for *TSMQR* to *UNMQR* + *TTMQR* it is 1.3032. Thus, we can expect about a 30% difference between the selection of the kernels since we will have instances of using in cache and out of cache throughout the run. Most of this difference is due to the higher efficiency and data locality within the *Triangle on top of square* kernels as compared to the *Triangle on top of triangle* kernels.

Having seen that the performance of the kernels can impact each of the algorithms, in order to provide a complete assessment of all of the current algorithms, we also compare the *Triangle on top of triangle* kernel algorithms to those using the *Triangle on top of square* kernels as shown in Figure **??**. For double precision, the observed difference in kernel speed is 4.976 GFLOP/sec for the *Triangle on top of square* kernels versus 3.844 GFLOP/sec for the *Triangle on top of triangle* kernels which provides a ratio of 1.2945 and is in accordance with our previous analysis. It can be seen that as the number of columns increases, whereby the amount of parallelism increases, the effect of the kernel performance outweighs the benefit provided by the extra parallelism afforded through the *Triangle on top of triangle* algorithms. Comparatively, in double complex precision, GREEDY does perform better, even against the algorithms using the *Triangle on top of square* kernels. As before, one must keep in mind that GREEDY does not require the tuning parameter of the domain size to achieve this better performance.

From these experiments, we showed that in double complex precision, GREEDY demonstrated better performance than any of the other algorithms and moreover, it does so without the need to specify a domain size as opposed to the algorithms in PLASMA. In addition, in double precision, for matrices where $p \gg q$, GREEDY continues to excel over any other algorithm using the *Triangle on top of triangle* kernels, and continues to do so as the matrices become more square.

5 Conclusion

In this paper, we have presented FIBONACCI, and GREEDY, two new algorithms for tiled QR factorization. These algorithms exhibit more parallelism than state-of-the-art implementations based on reduction trees. We have provided accurate estimations for the length of their critical path, and we have proven that they were asymptotically optimal for a wide class of matrix shapes, including all cases where the number of tile rows p and tile columns q are proportional, $p = \lambda q$, $\lambda \geq 1$. To the best of our knowledge, this proof is the first complexity result in the field of tiled algorithms, and it lays the theoretical foundations for a comparative study of these algorithms.

Comprehensive experiments on multicore platforms confirm the superiority of the new algorithms for $p \times q$ matrices, as soon as, say, $p \geq 2q$. This holds true when comparing not only with previous algorithms using TT (*Triangle*

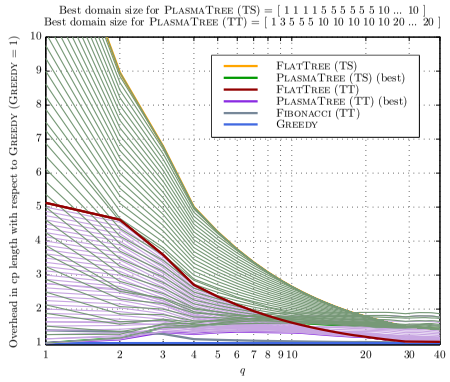

(a) Theoretical CP length

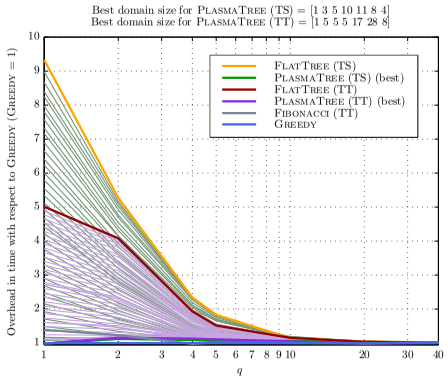

(b) Experimental (double complex)

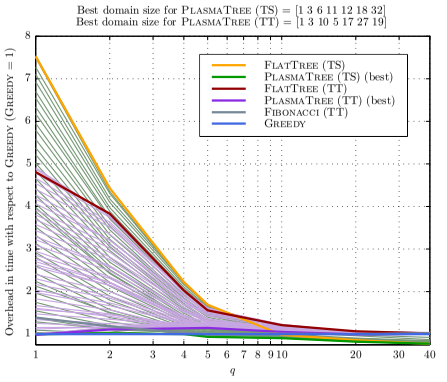

(c) Experimental (double)

FIGURE 6 – Overhead in terms of critical path length and time with respect to GREEDY (GREEDY = 1)

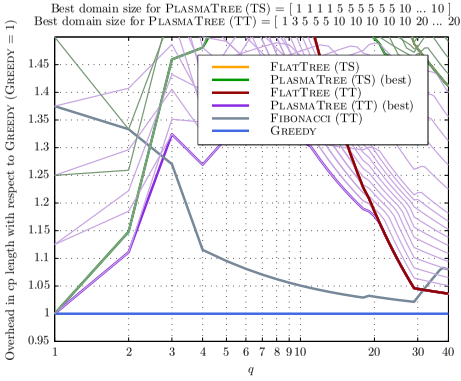

(a) Theoretical CP length

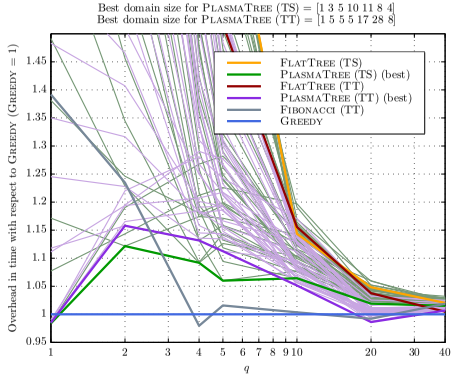

(b) Experimental (double complex)

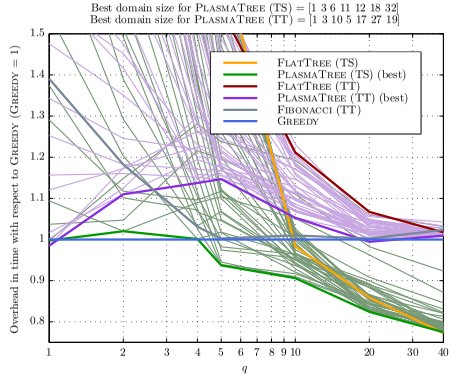

(c) Experimental (double)

FIGURE 7 – Detailed view of the overhead in terms of critical path length and time with respect to GREEDY (GREEDY = 1)

p	q	GREEDY	PLASMATREE (TT)	BS	Overhead	Gain	FIBONACCI	Overhead	Gain
40	1	16	16	1	1.0000	0.0000	22	1.3750	0.2727
40	2	54	60	3	1.1111	0.1000	72	1.3333	0.2500
40	3	74	98	5	1.3243	0.2449	94	1.2703	0.2128
40	4	104	132	5	1.2692	0.2121	116	1.1154	0.1034
40	5	126	166	5	1.3175	0.2410	138	1.0952	0.0870
40	6	148	198	10	1.3378	0.2525	160	1.0811	0.0750
40	7	170	226	10	1.3294	0.2478	182	1.0706	0.0659
40	8	192	254	10	1.3229	0.2441	204	1.0625	0.0588
40	9	214	282	10	1.3178	0.2411	226	1.0561	0.0531
40	10	236	310	10	1.3136	0.2387	248	1.0508	0.0484
40	11	258	336	20	1.3023	0.2321	270	1.0465	0.0444
40	12	280	358	20	1.2786	0.2179	292	1.0429	0.0411
40	13	302	380	20	1.2583	0.2053	314	1.0397	0.0382
40	14	324	402	20	1.2407	0.1940	336	1.0370	0.0357
40	15	346	424	20	1.2254	0.1840	358	1.0347	0.0335
40	16	368	446	20	1.2120	0.1749	380	1.0326	0.0316
40	17	390	468	20	1.2000	0.1667	402	1.0308	0.0299
40	18	412	490	20	1.1893	0.1592	424	1.0291	0.0283
40	19	432	512	20	1.1852	0.1562	446	1.0324	0.0314
40	20	454	534	20	1.1762	0.1498	468	1.0308	0.0299
40	21	476	554	20	1.1639	0.1408	490	1.0294	0.0286
40	22	498	570	20	1.1446	0.1263	512	1.0281	0.0273
40	23	520	586	20	1.1269	0.1126	534	1.0269	0.0262
40	24	542	602	20	1.1107	0.0997	556	1.0258	0.0252
40	25	564	618	20	1.0957	0.0874	578	1.0248	0.0242
40	26	586	634	20	1.0819	0.0757	600	1.0239	0.0233
40	27	608	650	20	1.0691	0.0646	622	1.0230	0.0225
40	28	630	666	20	1.0571	0.0541	644	1.0222	0.0217
40	29	652	682	20	1.0460	0.0440	666	1.0215	0.0210
40	30	668	698	20	1.0449	0.0430	688	1.0299	0.0291
40	31	684	714	20	1.0439	0.0420	710	1.0380	0.0366
40	32	700	730	20	1.0429	0.0411	732	1.0457	0.0437
40	33	716	746	20	1.0419	0.0402	754	1.0531	0.0504
40	34	732	762	20	1.0410	0.0394	776	1.0601	0.0567
40	35	748	778	20	1.0401	0.0386	798	1.0668	0.0627
40	36	764	794	20	1.0393	0.0378	820	1.0733	0.0683
40	37	780	810	20	1.0385	0.0370	842	1.0795	0.0736
40	38	796	826	20	1.0377	0.0363	862	1.0829	0.0766
40	39	812	842	20	1.0369	0.0356	878	1.0813	0.0752
40	40	826	856	20	1.0363	0.0350	892	1.0799	0.0740

TABLE 5 – GREEDY versus PLASMATREE (TT) and FIBONACCI (Theoretical)

p	q	GREEDY	PLASMATREE (TT)	BS	Overhead	Gain
40	1	36.9360	37.5020	1	1.0153	-0.0153
40	2	58.5090	52.7180	3	0.9010	0.0990
40	4	103.2670	90.7940	10	0.8792	0.1208
40	5	115.3060	100.5540	5	0.8721	0.1279
40	10	153.5180	145.8200	17	0.9499	0.0501
40	20	170.8730	171.8270	27	1.0056	-0.0056
40	40	184.5220	182.8160	19	0.9908	0.0092

TABLE 6 – GREEDY versus PLASMATREE (TT) (Experimenta Double)

p	q	GREEDY	PLASMATREE (TT)	BS	Overhead	Gain
40	1	42.0710	42.7120	1	1.0152	-0.0152
40	2	60.4420	52.1970	5	0.8636	0.1364
40	4	95.1820	84.1120	5	0.8837	0.1163
40	5	107.6370	96.7530	5	0.8989	0.1011
40	10	135.0270	128.4320	17	0.9512	0.0488
40	20	144.4010	146.4220	28	1.0140	-0.0140
40	40	152.9280	151.9090	8	0.9933	0.0067

TABLE 7 – GREEDY versus PLASMATREE (TT) (Experimental Double Complex)

p	q	GREEDY	FIBONACCI	Overhead	Gain
40	1	36.9360	26.5610	0.7191	0.2809
40	2	58.5090	49.4870	0.8458	0.1542
40	4	103.2670	100.1440	0.9698	0.0302
40	5	115.3060	115.0020	0.9974	0.0026
40	10	153.5180	152.0090	0.9902	0.0098
40	20	170.8730	170.4780	0.9977	0.0023
40	40	184.5220	180.2990	0.9771	0.0229

TABLE 8 – Greedy versus FIBONACCI (Experimental Double)

p	q	GREEDY	FIBONACCI	Overhead	Gain
40	1	42.0710	30.2280	0.7185	0.2815
40	2	60.4420	48.9570	0.8100	0.1900
40	4	95.1820	97.1650	1.0208	-0.0208
40	5	107.6370	105.9610	0.9844	0.0156
40	10	135.0270	134.5500	0.9965	0.0035
40	20	144.4010	145.5530	1.0080	-0.0080
40	40	152.9280	150.0980	0.9815	0.0185

TABLE 9 – GREEDY versus FIBONACCI (Experimental Double Complex)

on top of triangle) kernels, but also with all known algorithms based on TS (*Triangle on top of square*) kernels. Given that TS kernels offer more locality, and benefit from better elementary arithmetic performance, than TT kernels, the better performance of the new algorithms is even more striking, and further demonstrates that a large degree of a parallelism was not exploited in previously published solutions.

Future work will investigate several promising directions. First, using rectangular tiles instead of square tiles could lead to efficient algorithms, with more locality and still the same potential for parallelism. Second, refining the model to account for communications, and extending it to fully distributed architectures, would lay the ground to the design of MPI implementations of the new algorithms, unleashing their high level of performance on larger platforms. Finally, the design of robust algorithms, capable of achieving efficient performance despite variations in processor speeds, or even resource failures, is a challenging but crucial task to fully benefit from future platforms with a huge number of cores.

Références

[1] E. Agullo, J. Dongarra, R. Nath, and S. Tomov. A fully empirical autotuned dense QR factorization for multicore architectures. Technical Report 242, LAPACK Working Note, Mar. 2011.

[2] E. Agullo, B. Hadri, H. Ltaief, and J. Dongarra. Comparative study of one-sided factorizations with multiple software packages on multi-core hardware. In *Proceedings of the Conference on High Performance Computing Networking, Storage and Analysis (SC '09)*, pages 1–12. IEEE Computer Society Press, 2009.

[3] S. Blackford and J. J. Dongarra. Installation guide for LAPACK. Technical Report 41, LAPACK Working Note, June 1999. originally released March 1992.

[4] A. Buttari, J. Langou, J. Kurzak, and J. Dongarra. Parallel tiled QR factorization for multicore architectures. *Concurrency Computat. : Pract. Exper.*, 20(13) :1573–1590, 2008.

[5] A. Buttari, J. Langou, J. Kurzak, and J. Dongarra. A class of parallel tiled linear algebra algorithms for multicore architectures. *Parallel Computing*, 35(1) :38–53, 2009.

[6] M. Cosnard, J.-M. Muller, and Y. Robert. Parallel QR decomposition of a rectangular matrix. *Numerische Mathematik*, 48 :239–249, 1986.

[7] M. Cosnard and Y. Robert. Complexity of parallel QR factorization. *Journal of the A.C.M.*, 33(4) :712–723, 1986.

[8] J. W. Demmel, L. Grigori, M. Hoemmen, and J. Langou. Communication-avoiding parallel and sequential QR and LU factorizations : theory and practice. Technical Report arXiv :0806.2159, 2008.

[9] B. Hadri, H. Ltaief, E. Agullo, and J. Dongarra. Enhancing parallelism of tile QR factorization for multicore architectures, 2009.

[10] B. Hadri, H. Ltaief, E. Agullo, and J. Dongarra. Tile QR factorization with parallel panel processing for multicore architectures. In *IPDPS'10, the 24st IEEE Int. Parallel and Distributed Processing Symposium*, 2010.

[11] J. Kurzak, H. Ltaief, J. Dongarra, and R. M. Badia. Scheduling dense linear algebra operations on multicore processors. *Concurrency and Computation : Practice and Experience*, 22(1) :15–44, 2010.

[12] J. Modi and M. Clarke. An alternative Givens ordering. *Numerische Mathematik*, 43 :83–90, 1984.

[13] G. Quintana-Ortí, E. S. Quintana-Ortí, R. A. van de Geijn, F. G. V. Zee, and E. Chan. Programming matrix algorithms-by-blocks for thread-level parallelism. *ACM Transactions on Mathematical Software*, 36(3).

[14] A. Sameh and D. Kuck. On stable parallel linear systems solvers. *J. ACM*, 25 :81–91, 1978.

[15] SimGrid. URL : http://simgrid.gforge.inria.fr.

[16] R. C. Whaley and A. M. Castaldo. Achieving accurate and context-sensitive timing for code optimization. *Softw. Pract. Exper.*, 38 :1621–1642, December 2008.

[17] S. Williams, A. Waterman, and D. Patterson. Roofline : an insightful visual performance model for multicore architectures. *Commun. ACM*, 52 :65–76, April 2009.

Centre de recherche INRIA Grenoble – Rhône-Alpes
655, avenue de l'Europe - 38334 Montbonnot Saint-Ismier (France)

Centre de recherche INRIA Bordeaux – Sud Ouest : Domaine Universitaire - 351, cours de la Libération - 33405 Talence Cedex
Centre de recherche INRIA Lille – Nord Europe : Parc Scientifique de la Haute Borne - 40, avenue Halley - 59650 Villeneuve d'Ascq
Centre de recherche INRIA Nancy – Grand Est : LORIA, Technopôle de Nancy-Brabois - Campus scientifique
615, rue du Jardin Botanique - BP 101 - 54602 Villers-lès-Nancy Cedex
Centre de recherche INRIA Paris – Rocquencourt : Domaine de Voluceau - Rocquencourt - BP 105 - 78153 Le Chesnay Cedex
Centre de recherche INRIA Rennes – Bretagne Atlantique : IRISA, Campus universitaire de Beaulieu - 35042 Rennes Cedex
Centre de recherche INRIA Saclay – Île-de-France : Parc Orsay Université - ZAC des Vignes : 4, rue Jacques Monod - 91893 Orsay Cedex
Centre de recherche INRIA Sophia Antipolis – Méditerranée : 2004, route des Lucioles - BP 93 - 06902 Sophia Antipolis Cedex

Éditeur
INRIA - Domaine de Voluceau - Rocquencourt, BP 105 - 78153 Le Chesnay Cedex (France)
http://www.inria.fr
ISSN 0249-6399